PROCEEDINGS OF THE ROYAL SOCIETY B BIOLOGICAL SCIENCES

Visual extrapolation under risk: human observers estimate and compensate for exogenous uncertainty

Paul A. Warren, Erich W. Graf, Rebecca A. Champion and Laurence T. Maloney

Proc. R. Soc. B published online 1 February 2012
doi: 10.1098/rspb.2011.2527

PROCEEDINGS OF THE ROYAL SOCIETY B

FirstCite® e-publishing

Proc. R. Soc. B
doi:10.1098/rspb.2011.2527
Published online

Visual extrapolation under risk: human observers estimate and compensate for exogenous uncertainty

Paul A. Warren[1,*], Erich W. Graf[2], Rebecca A. Champion[1] and Laurence T. Maloney[3]

[1]*School of Psychological Sciences, University of Manchester, Manchester M13 9PL, UK*
[2]*School of Psychology, University of Southampton, Southampton SO17 1BJ, UK*
[3]*Department of Psychology, Center for Neural Science, New York University, New York, NY 10003, USA*

Humans commonly face choices between multiple options with uncertain outcomes. Such situations occur in many contexts, from purely financial decisions (which shares should I buy?) to perceptuo-motor decisions between different actions (where should I aim my shot at goal?). Regardless of context, successful decision-making requires that the uncertainty at the heart of the decision-making problem is taken into account. Here, we ask whether humans can recover an estimate of exogenous uncertainty and then use it to make good decisions. Observers viewed a small dot that moved erratically until it disappeared behind an occluder. We varied the size of the occluder and the unpredictability of the dot's path. The observer attempted to capture the dot as it emerged from behind the occluded region by setting the location and extent of a 'catcher' along the edge of the occluder. The reward for successfully catching the dot was reduced as the size of the catcher increased. We compared human performance with that of an agent maximizing expected gain and found that observers consistently selected catcher size close to this theoretical solution. These results suggest that humans are finely tuned to exogenous uncertainty information and can exploit it to guide action.

Keywords: exogenous uncertainty; maximum expected gain; cue combination; statistical approaches; motion extrapolation; decision under risk

1. INTRODUCTION

In crossing a busy road, the prudent pedestrian attempts to predict the future positions of cars and other vehicles, and plans a path to avoid them. In the laboratory, human ability to extrapolate the path of objects in motion is impressive over a variety of conditions; observers can accurately track objects through visual noise [1,2] or after a period of occlusion [3]. Motion extrapolation can occur with or without tracking eye movements [4]; when imagining a target [5]; or while expecting a target to reappear after occlusion [6,7]. During occlusion, smooth pursuit continues, albeit with reduced gain and eye velocity [7].

The pedestrian's decision whether to act on the plan, though, should also reflect the uncertainty in extrapolation and, ultimately, the probability that this plan will lead the pedestrian safely to the other side of the street. If it is dark or rainy, then a decision not to cross might be best precisely because of increased uncertainty in the prediction.

In the last decade, researchers in the field of human perception and action have begun to investigate decision tasks where perceptual and motor uncertainty play critical roles. In these tasks, observers plan a movement, execute it and receive monetary rewards or penalties determined by the outcome of the movement (for review, see [8,9]). The outcomes ranged from hitting a target on a computer monitor [10–12], arriving at a goal in a specified time window [13], trading off speed and accuracy [14] or speed and information [15], or planning a series of movements [16,17]. Observers could maximize their expected gain (EG) only if they compensated for their own visual and motor uncertainty in planning movements. Participants in these movement-planning tasks typically (but not always) planned movements that came close to maximizing their EG. In doing so, they demonstrated that they—like the prudent pedestrian—take into account uncertainty in planning movement (in this case, their own motor and visual uncertainty).

In most of the studies just mentioned, the participants' endogenous visual and motor 'noise' was the dominant source of uncertainty. The pedestrian, though, confronts an additional, exogenous uncertainty. The future locations of vehicles on roads are effectively stochastic because drivers can change direction and velocity in unpredictable ways.

In this article, we use a gambling task to investigate human ability to extrapolate the paths of objects engaged in a 'random walk', the future paths of which are only partly predictable. Observers can succeed in maximizing EG only if they correctly model the uncertainty intrinsic to the movement of the object whose path is extrapolated. We test whether human observers can model exogenous uncertainty and whether they can use this information to make good decisions.

* Author for correspondence (paul.warren@manchester.ac.uk).

Electronic supplementary material is available at http://dx.doi.org/10.1098/rspb.2011.2527 or via http://rspb.royalsocietypublishing.org.

Received 2 December 2011
Accepted 11 January 2012

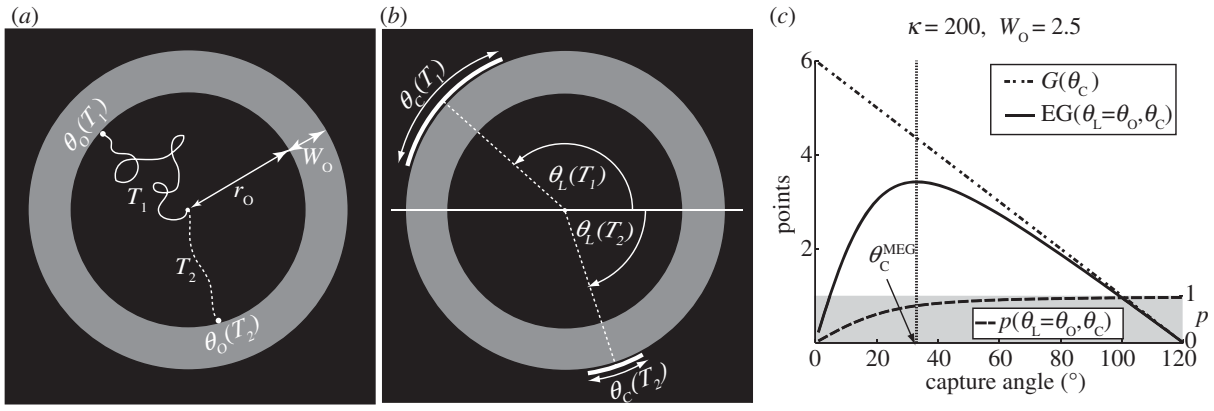

Figure 1. Task and notation. (*a*) The participant first viewed a small dot that moved outward from the centre of a circular arena along a stochastic trajectory until it disappeared under an occluder (grey ring) with inner radius r_O and width W_O. Two examples of trajectories (T_1 and T_2) are shown. Only the moving dot was visible to the observer, not the static trajectory as drawn here. After the dot reached the occluder, it stopped, marking the point of occlusion (r_O, θ_O) in polar coordinates. The dot remained visible for the remainder of the trial. (*b*) The observer then set the *location* (θ_L) and *width* (θ_C) of a circular segment (a 'catcher') intended to 'capture' the dot as it re-emerged from behind the occluder. Two examples of catchers are shown. If the dot reappeared within the circular segment marked by the catcher, then the participant earned a reward (gain) G and otherwise received nothing. (*c*) The probability of capture, $p(\theta_L, \theta_C)$, depends on both the location θ_L and width θ_C of the observer's setting of the catcher. We plot an example of $p(\theta_L, \theta_C)$ as a function of θ_C for the special case $\theta_L = \theta_O$ (the observer has centred the catcher on the point of occlusion θ_O). The probability of capture $p(\theta_L, \theta_C)$ increases with capture angle θ_C (dashed line). In the experiment, the magnitude of the reward G was determined by the experimenter and it decreased with the width θ_C of the catcher. An example of $G(\theta_C)$ versus θ_W is plotted as a dash-dotted line. $EG(\theta_L, \theta_C) = p(\theta_L, \theta_C)G(\theta_C)$ is plotted versus θ_C (solid line). The choice of catcher width θ_C maximizing the observer's EG (for the choice of $\theta_L = \theta_O$ used throughout this example) is marked with a dotted vertical line. In general, EG depended on both the observer's settings of the location θ_L and capture angle θ_C of the catcher.

The key aspects of the extrapolation task used in the present study are shown in figure 1. This approach has similarities to that used by Graf *et al.* [18]; however, in the present study, we incorporate a new risky decision-making task. Participants observe a circular *arena* and a small dot travelling on an irregular and unpredictable path outward from a central starting point (two such possible trajectories, T_1 and T_2, are shown in figure 1*a*, with T_2 less irregular than T_1). The dot disappears when it hits the occluder at point (r_O, θ_O) and the observer must adjust a circular segment (the 'catcher') to attempt to 'capture' the dot when it reappears on the outside on the occlusion region (figure 1*b*).[1]

The observer is free to adjust both the *location* θ_L of the centre of the catcher around the perimeter of the occluder and the *angular extent* of the catcher θ_C. Once the observer has completed the setting, the point where the dot re-emerged is shown. If the dot re-emerges within the span of the catcher, the observer receives a monetary reward; otherwise, no reward is received.

The probability that the adjusted catcher will capture the dot, $p(\theta_L, \theta_C)$, is an increasing function of θ_C because for any fixed choice of θ_L the probability of catching the dot cannot decrease as the angular extent of the catcher is increased. To illustrate this point, in figure 1*c*, we plot $p(\theta_L, \theta_C)$ versus θ_C (dashed line) for the special case where $\theta_L = \theta_O$; that is, the observer has centred the catcher on the angular coordinate where the dot disappeared beneath the occluder. The function is increasing: the greater the angular extent of the catcher, the greater the chances the dot will be caught.

An observer wishing to simply capture the dot would set the catcher to its maximum width. However, in our experiment, the gain received for a successful capture depends on the observer's choice of capture angle, θ_C: the smaller the width of the catcher, the greater the reward (gain), $G(\theta_C)$. We plot $G(\theta_C)$ versus θ_C in figure 1*c* (dash-dotted line) for one of the conditions of our experiment.

The EG for any setting of the catcher (θ_L, θ_C) is then

$$EG(\theta_L, \theta_C) = p(\theta_L, \theta_C)\, G(\theta_C), \tag{1.1}$$

plotted in figure 1*c* for the special case $\theta_L = \theta_O$ (solid line).

As θ_C changes, there is an evident trade-off between the probability of getting a reward and the amount of reward obtained. We verified computationally that there is a unique point $(\theta_L^{MEG}, \theta_C^{MEG})$ that maximizes EG in each of our experimental conditions. This setting θ_C^{MEG}, for the hypothetical case where the observer centres the catcher on the point of occlusion $(\theta_L = \theta_O)$, is marked with a vertical dotted line in figure 1*c*. We compare human performance with ideal performance maximizing EG. We postpone discussion of how to compute the maximum expected gain (MEG) solution until after we describe the algorithm used to generate the stimuli in §2*a*.

2. EXPERIMENT

(a) *Methods*

(i) *Observers*

All observers were students or staff at Cardiff University and all took part in the experiment under informed consent. There were five observers, none of whom was aware of the hypotheses under test.

(ii) *Apparatus*

Stimuli were presented on a 22-inch flat-screen Viewsonic p225f CRT display (1024×768 pixels; $40 \times 30^\circ$). Observers sat approximately 57.3 cm from the monitor

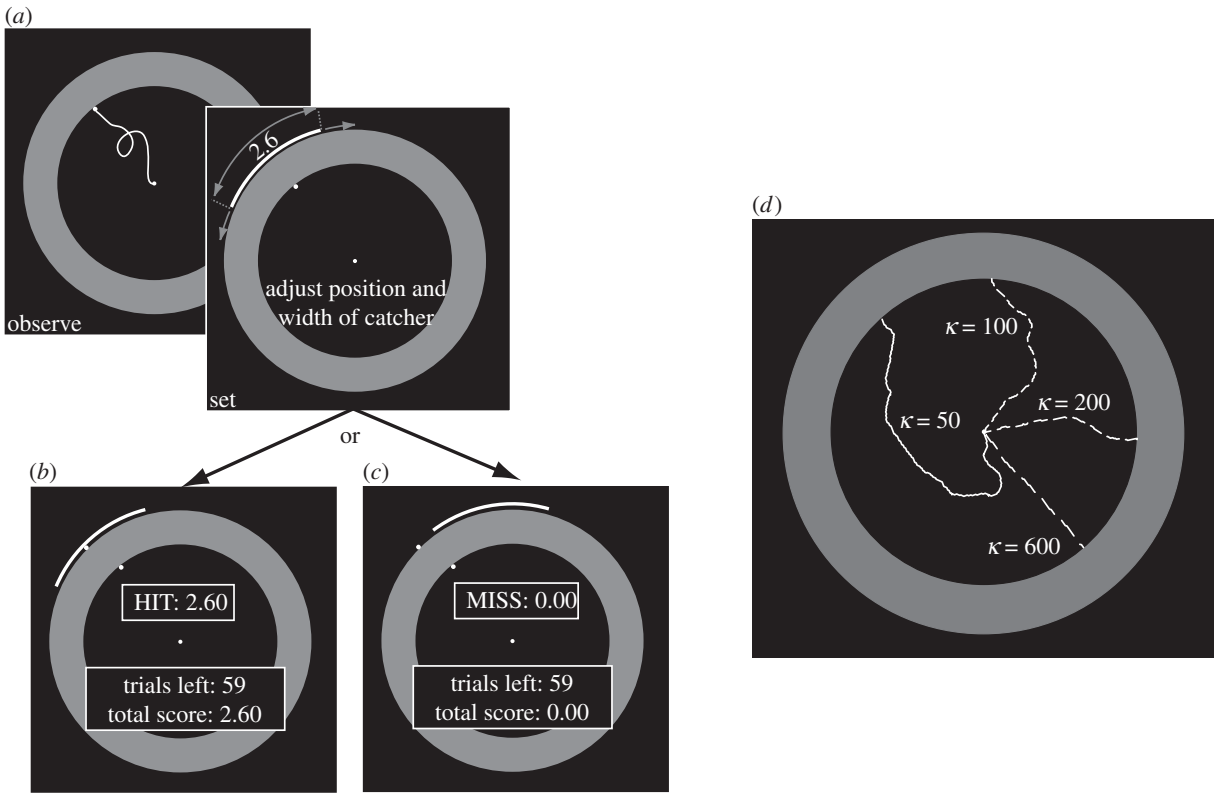

Figure 2. Sequence of events on a single trial. (*a*) Observe and set: the observer saw the dot move along a trajectory and disappear behind an occluder. The point of occlusion was marked by a dot that remained on the screen for the remainder of the trial. The observer then set the location and width of the catcher. As the observer varied the width, the reward in points associated with 'catching' the point was displayed on the screen near the catcher. (*b*,*c*) Feedback: a second dot appeared, marking the point at which the dot re-emerged from behind the occluder. The reward earned by the observer for that trial was also displayed. If the point of re-emergence fell within the catcher, the observer received the reward G determined by the width of the catcher (*b*); otherwise, zero reward (*c*). At the end of the experiment, the observer received a bonus proportional to the total of points earned (see text). (*d*) Examples of paths generated with the four values of directional reliability κ used in the experiment.

and viewed the display binocularly. The centre of the screen was approximately at eye level.

(iii) *Task*

The task is schematically presented in figure 2. Observers watched a dot travel towards the inner edge of the occluder, at which point it stopped (figure 2*a*; note that the motion trail is presented for illustration purposes only and was not given in the experiment). Observers were then asked to try to 'catch' the dot when it emerged outside the occluder using an arc segment whose position and angular extent (the capture angle) could be varied—the 'catcher' described above (figure 2*a*). As the capture angle varied, so did the number of points that the observer could score if they caught the dot and the points. The points that could be won were presented adjacent to the catcher (figure 2*a*) and varied as the observer varied the width of the catcher.

The points scored if the dot was caught varied as a linear function of angular arc length from a minimum of 0.05 points when the arc length was 120° to a maximum of six points when the arc length was 1° (figure 1*c*, dash-dotted line). The maximum possible arc length was constrained to be 120°, and in practice observers never set the arc length to be this large.

Observers took on the order of 1–2 s to set the arc length. After the observer completed the setting, the position of the dot when it exited from behind the outer edge of the occluder was shown. If the final position of the dot on the outer edge of the occluder fell within the catcher set by the observer, then the catcher turned green, the observer was informed that they had caught the dot (HIT) and the associated points were awarded (figure 2*b*). If it did not, the catcher turned red, the observer was informed they had missed the dot (MISS) and no points were awarded (figure 2*c*).

(iv) *Instructions*

Observers were simply instructed to score as many points as possible during the experiment by catching the dot. We measured the observers' settings of θ_L and θ_C on each trial. We attempted to increase observers' motivation by awarding a bonus prize for the observer who scored the most points.

(v) *Stimuli*

The visual stimulus consisted of a single red dot moving on a random walk trajectory from the centre of the screen towards the inner edge of a grey annulus occluder on an otherwise blank screen (figure 1*a*). The distance from the start point to the inner edge of the occluder was $r_O = 6.5°$. On a given trial, the dot moved at a constant speed s in a direction that changed at discrete

temporal intervals synchronized with the frame rate of the CRT (100 Hz).

(vi) *The von Mises random walk*

The changes in direction were random variables drawn from a von Mises distribution [19] with mean 0° ('straight ahead'). The variability of the random walk was controlled by a parameter κ. We refer to κ as the *directional reliability* of the motion path. Trials with low values of κ typically had more erratic paths than trials with high values. Figure 2*d* shows examples of paths that might be obtained when sampling from distributions with the values of κ that we used in the experiment (for more details on the random walk process, see the electronic supplementary material).

When the dot reached the edge of the arena, we stopped the updating process and allowed the observer to set the catcher as described earlier. The observer was then shown the point at which the dot re-emerged from behind the occluder as determined by continuing the updating process. Note that, while unlikely, it was possible that the dot would pass back and forth from the occluder region to the central arena one or more times before finally emerging on the outside of the occluder. The observer received a reward only if the dot first reached the outer edge of the occluder within the catcher set by the observer. Note the distance between the inner edge of the occluder and the centre of the arena is fixed in all trials. The state vector of the dot when it reaches the edge of the occluder is (x_O, y_O, v_O), where x_O and y_O represent the dot position, and v_O the instantaneous dot direction at occlusion. We may then represent the coordinates (x_O, y_O) in polar coordinates as (r_O, θ_O), as shown in figure 1*a*. Then, because r_O is a constant, the distribution of future paths of the point under the occluder is determined by (θ_O, v_O).

(vii) *Design*

The independent variables were the κ parameter (50, 100, 200 and 600) illustrated in figure 2*d*; the occluder width, W_O (1, 2.5, 4 cm); and the speed of the dot, s (1.5, 3.0 deg s^{-1}). They were combined in a full factorial repeated-measures design to give 24 conditions. Observers undertook six repetitions of each of the 24 conditions in randomized order.

(viii) *Dependent measures*

We measured the position (θ_L), and capture angle (θ_C) of the capture region on each trial.

(ix) *Statistical analysis*

All capture angles are limited to between 0° and 120°. Because there is no danger of wrap-around, we report linear (rather than circular) descriptive statistics and conduct linear statistical analyses.

3. RESULTS

(a) *Initial analysis*

We conducted a preliminary three-factor repeated-measures ANOVA on the data. In a previous study, we had found no effect of speed and thus were able to collapse across this condition. In the present study, we found a similar pattern of results at the group level ($F_{1,4} = 0.874$, $p > 0.05$), and at the level of the individual observer (all $p > 0.05$ after Bonferroni correction; see electronic supplementary material). Therefore, our subsequent analyses have been conducted on the data collapsed across speed with effectively 12 distinct experimental conditions (4 directional reliabilities; $\kappa \times 3$ occluder widths, W_O).

(b) *Point estimate data*

The observer's choice of θ_L, the location of the capture region, can be treated as a point estimate of where the dot will emerge from behind the occluder. We will not focus on this aspect of the data in detail. Observers tend to centre the catcher at the angle θ_O, at which the dot hit the inner edge of the occluder.

In figure 3, we plot histograms of the deviations $\theta_L - \theta_O$ of each setting from θ_O for each of the 12 conditions. As can be seen, in all conditions, the data are well described by a Gaussian distribution centred on 0 and with the same standard deviation as the data in the corresponding condition. The fitted distributions have relatively small standard deviations (the largest is approx. 17°).

This pattern may be expected given the information available to observers when setting θ_L: they could see both the centre point of the arena, and the position of the dot as it hit the inner edge of the occluder. The observed data could result from a strategy of extending an imaginary line from the centre of the arena, through the point at which the dot entered the occluder to the outer occluder edge. Such a strategy would appear to not use information that might be obtained from the dot direction at the point where it hit the occluder; we will test for evidence of this in §3*c*.

(c) *Prediction of catcher location settings*

The distribution of future paths of the dot is determined by the state vector (θ_O, v_O) specifying where the dot reached the occluder and its instantaneous direction when it did so. Thus, if the dot was 'turning' clockwise or anti-clockwise as it reached the occluder, then it is possible that an observer might compensate by adjusting the location of the catcher clockwise or anti-clockwise. In effect, would a regression model with both θ_O and v_O better predict θ_L than θ_O by itself?

To test for this possibility, we performed a linear regression analysis of setting θ_L on the independent variables θ_O and $\Delta v_O = v_O - \theta_O$. The latter independent variable is the deviation of v_O away from θ_O. We found no significant effect of Δv_O on setting θ_L ($t_{597} = -1.219$; $p = 0.224$), but a highly significant effect of θ_O on setting θ_L ($t_{597} = 170.701$; $p < 0.0001$). The intercept term was not significantly different from 0 ($t_{597} = -0.710$; $p = 0.478$); that is, observers' settings were not biased away from θ_O. The overall $r^2 = 0.989$ was high. The same regression analysis was also performed on each observer's data independently, with the same pattern of results for all observers (details given in the electronic supplementary material).

These outcomes are consistent with the claim that v_O did not affect observers' settings. Accordingly, we assume that observers set the location of the catcher θ_L to match θ_O and did not make use of an estimate of v_O, the direction the point was travelling when it reached the occluder. This outcome is perhaps not surprising because θ_O was marked with a visible red dot that remained on the screen during the setting, whereas v_O (the direction of the last segment of the random walk) was difficult to estimate from the available visual

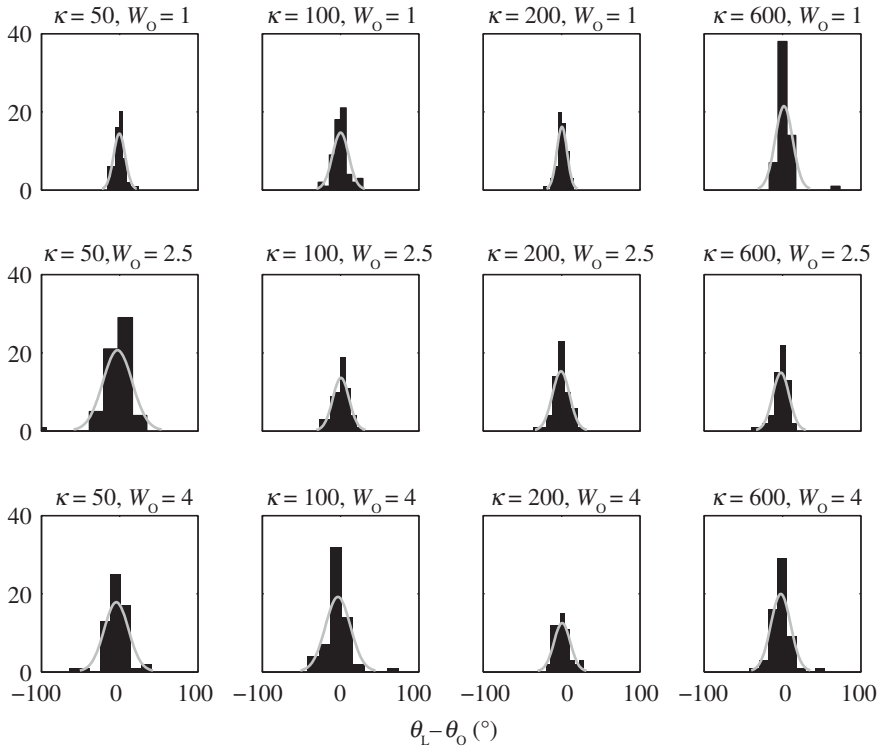

Figure 3. Location settings. Histograms of $\theta_L - \theta_O$ for all 12 conditions of the experiment (four values of κ crossed with three occluder widths W_O, collapsed across speed; see text). The histograms are roughly Gaussian in form, centred on 0. Gaussian probability densities centred on 0 and matched in standard deviation to the data of the corresponding condition are shown as grey curves superimposed on the histograms.

evidence. It is also possible that the strategy was a consequence of a decrease in the reliability of the observer's estimate of dot direction across the duration of the setting (although Graf *et al.* [18] have suggested that observers are able to accumulate and store trajectory information over periods lasting several seconds).

(d) *Interval estimate data*

In figure 4*a*, we plot the average capture angle (θ_C) across observers versus directional reliability κ for each W_O. We can see from figure 4*a* (symbols) that as the path becomes more unreliable, the observers tend to make the capture angle bigger. Similarly, when occluder width W_O is increased observers tend to set the capture angle to be bigger. The effects of both reliability κ ($F_{3,12} = 6.511$, $p < 0.01$) and W_O ($F_{2,8} = 8.553$, $p = 0.01$) are significant, but there is no significant interaction between these variables ($F_{6,24} = 0.425$, $p > 0.05$). These data suggest that observers take both directional reliability and W_O into account in selecting a capture angle. This in itself is not necessarily surprising—it would not be sensible to set the catcher smaller as the path became more variable or the W_O increased. However, we want to know whether observers are able to model the variability appropriately (i.e. do they know precisely how much more or less variable one path is than another?).

To address this question, we used Monte Carlo methods. For each of the 12 conditions of the experiment, we simulated 100 trajectories up to the occluder and, for each of these, calculated a further 1000 trajectories under the occluder (i.e. 100 000 trajectories in total per condition). For each of the 100 up to occluder trajectories, we calculated the circular standard deviation, $\sigma_i^{\text{exit}}(\kappa, W_O)$, $i = 1, 2, \ldots, 100$ of the exit distribution over the 1000 under occluder trajectories [20]. We then took the circular average of the $\sigma_i^{\text{exit}}(\kappa, W_O)$ over the 100 up to occluder trajectories. This resulted in a single trajectory variability estimate, $\bar{\sigma}^{\text{exit}}(\kappa, W_O)$, for each of the experimental conditions. This approach is similar to that used by Graf *et al.* [18]. In doing so, we averaged out the effect of differences in the direction of the dot when it hit the occluder, v_O, on the subsequent setting (because each of the 100 up to occluder trajectories would have a different v_O). However, as discussed earlier, this parameter has little additional influence on the setting beyond that of the position θ_O at which the dot hits the occluder. Nonetheless, we maintain this approach because it ensures that the trajectories simulated and the subsequent calculations of $\bar{\sigma}^{\text{exit}}(\kappa, W_O)$ take into account the possible variability in v_O.

We reasoned that if observers could recover the variability in the trajectory, then their settings should be tightly correlated with the $\bar{\sigma}^{\text{exit}}(\kappa, W_O)$ values obtained from the simulations. We fitted the data to a model

$$\theta_C = \alpha(\sigma^{\text{exit}})^{\beta} W_O^{\gamma} \tag{3.1}$$

which includes a term W_O. The actual fits were performed by a linear regression on the variables transformed by a natural logarithm

$$\log \theta_C = \log \alpha + \beta \log \bar{\sigma}^{\text{exit}} + \gamma \log W_O. \tag{3.2}$$

The results of the regression are presented in figure 4*b*. We find a strong relationship ($r^2 = 0.915$) between $\bar{\sigma}^{\text{exit}}$

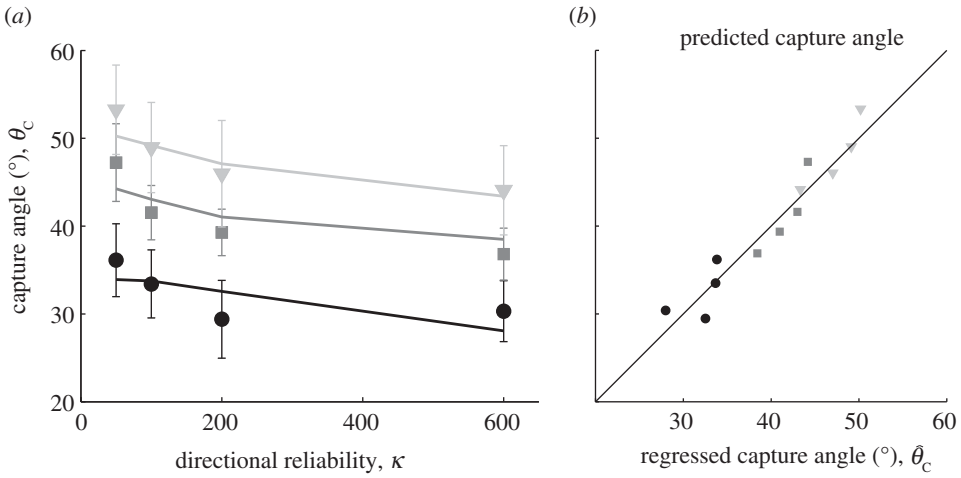

Figure 4. Capture angle settings. (*a*) Mean capture angle across observers in the 12 different conditions studied. Error bars mark ± 1 s.e. The solid curves are the predicted settings for the regression model described in the text. $W_O = 1$ (circles), $W_O = 2.5$ (squares) and $W_O = 4$ cm (triangles). (*b*) The mean catcher width across observers regressed against the standard deviation of the simulated exit distributions in the Monte Carlo analysis described in the text.

and observed capture angle with regressed capture angle averaged across observers given by:

$$\hat{\theta}_C = 75.79(\sigma^{exit})^{0.084} W_O^{0.225}. \quad (3.3)$$

The regressed capture angles are superimposed on the plot of observed capture angle versus von Mises parameter κ in figure 4*a* (lines) and the regression is reported in figure 4*b*.

The resulting fit is close to the data except at the smallest value of κ, suggesting that equation (3.1) is only approximate. In the electronic supplementary material, we report further analyses of these data, which suggest that the correct functional form for equation (3.1) is closer to a straight line than a power transformation over the range of W_O employed in the actual experiment.

We conclude that the quantity that observers are encoding and reporting when making a capture angle setting is tightly coupled to a quantity reflecting the objective variability in the path directly. The next question to address is whether observers can use this variability information to make good decisions.

To investigate this question, we used similar Monte Carlo methods (described in the electronic supplementary material) to simulate two ideal observer models for estimation of the capture angle θ_C^{MEG} that would maximize EG in each of the 12 conditions. The two models (referred to as the *stochastic setting model* and the *exact setting model*) differed in two respects. The exact setting model used the information about direction of motion v_O on the last time step before occlusion to set the location of the catcher. Specifically, the catcher was always centred at the point where the dot would have emerged from behind the occluder if it had continued moving in direction v_O. In contrast, the stochastic setting model did not use v_O (as was the case for our observers). Furthermore, the stochastic setting model took into account the observer's uncertainty in setting the location of the catcher (figure 3), whereas in the exact setting model the observer's setting uncertainty was 0. The stochastic setting model is therefore a more realistic, cognitively bounded [21] model of human performance, whereas the exact setting model corresponds to an upper bound on human performance.

For both models, we used a Monte Carlo approach similar to that described earlier (see electronic supplementary material) to recover probability profiles for each θ_C in each condition. All profiles were monotonically increasing as expected. We then computed the $EG(\theta_C)$ using equation (1.1) for both ideal observer models. The capture angle settings that would maximize EG for each condition were then obtained from:

$$\theta_C^{MEG} = \arg\max_{\theta_C} EG(\theta_C). \quad (3.4)$$

We verified computationally, for both models, that the resultant expected value curves were unimodal, so there is a single maximum expected gain (MEG) solution that determines the best capture angle to use. The expected value curve for the stochastic setting model is shown in figure 5*a* (unbroken curve). The value of θ_C^{MEG} and the associated MEG for the exact setting model are also shown (dashed vertical and horizontal lines). The value of θ_C^{MEG} for the stochastic setting model is indicated by an unbroken vertical black line. The mean capture angle θ_C and EG for each of our five observers is also shown (grey circles), together with the average across observers (white circle, vertical grey line).

Clearly, our observers' capture angle settings (both on average and for the most part individually) were larger than the solutions predicted by the exact setting model MEG solution. Consequently, human performance is considerably worse than this model. This is not surprising; as demonstrated earlier (and in the electronic supplementary material), our observers did not take into account the direction of dot movement on the final step before occlusion. However, in all 12 conditions, the average capture angle obtained across observers is remarkably close to the stochastic setting model MEG solution, with root mean square error over conditions of around 3°.

These findings are supported by the expected efficiency data. In figure 5*b*, we plot expected efficiency, calculated as the expected points scored for each observer based on their capture angle as a percentage of the points

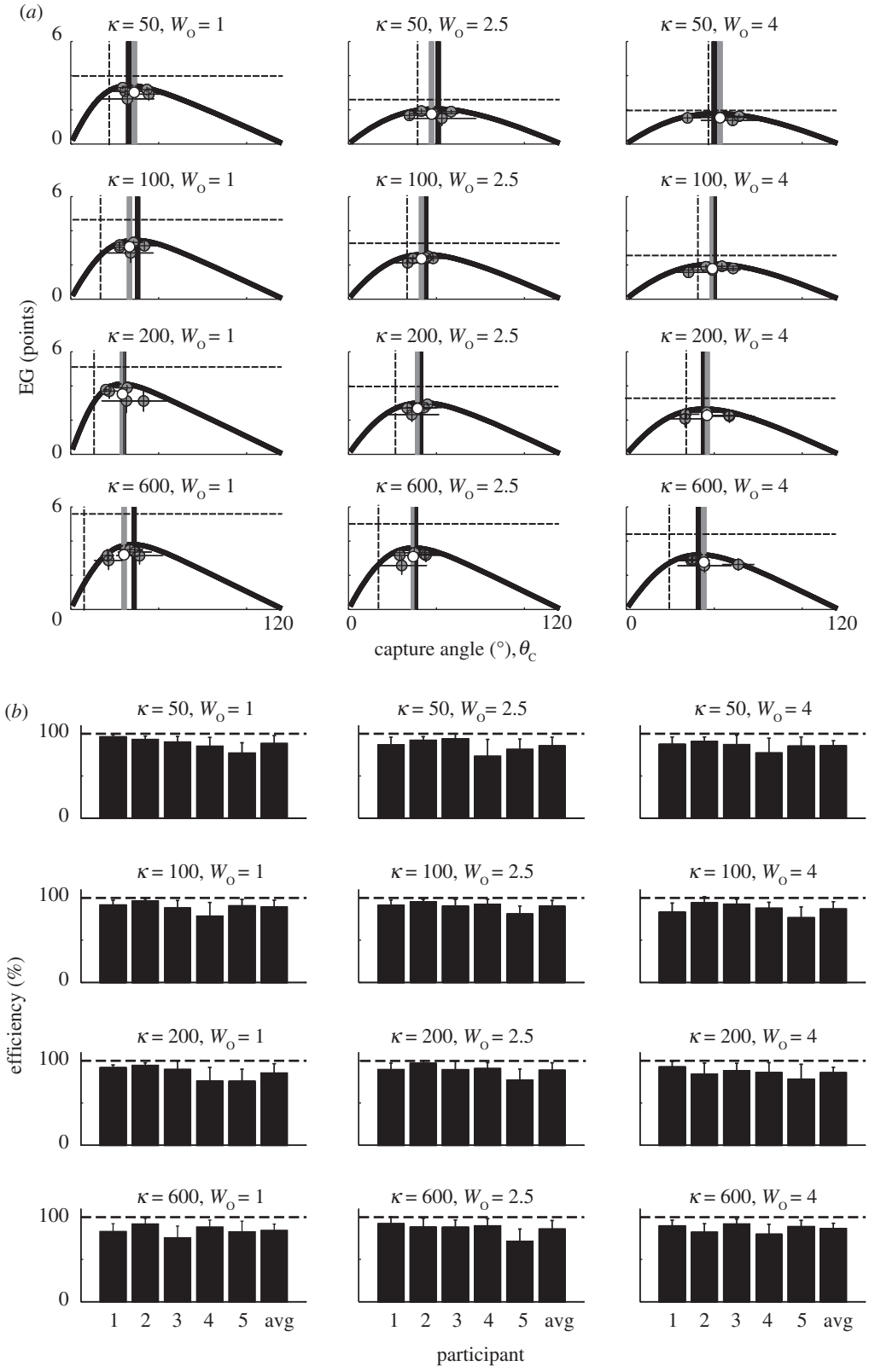

Figure 5. (*a*) Expected gain (EG) curves generated by multiplying the p_C (shown in the electronic supplementary material, figure S3) by the points that would be scored for a successful catch at each capture angle. The maximum of each curve is marked by a black vertical line. This maximum corresponds to the setting of the occluder maximizing expected gain (MEG) in the corresponding experimental condition. Mean trial-by-trial EGs are plotted against mean capture angle for each observer, shown as grey circles (error bars denote 95% confidence intervals). The mean capture angle across observers is marked by a grey vertical line and the mean EG across observers for this capture angle is shown as a white circle. The dashed black lines correspond to the MEG predictions of the exact setting model (see text). (*b*) Expected efficiency for the observed capture angles in each of the 12 experimental conditions for each of the five observers individually and for the average over observers (avg). Error bars for each observer represent 95% confidence intervals, whereas error bars for the average observer are $\pm$ 1 s.e.

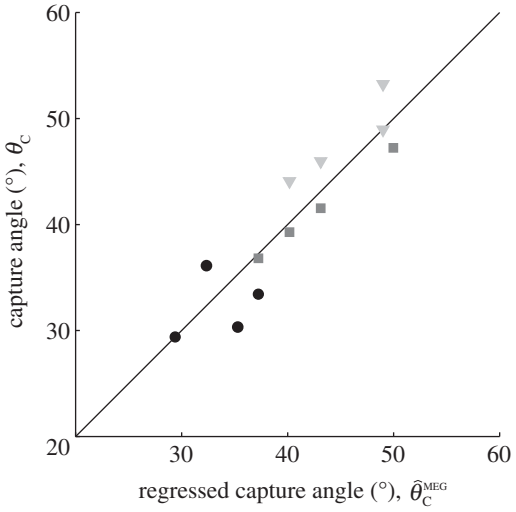

Figure 6. A plot of $\hat{\theta}_C^{MEG}$ (the regressed capture angle obtained by regressing θ_C^{MEG}) against the observed capture angles (parameter values arising from the fits are described in the text). Values for different occluder widths (W_O) are plotted in distinct symbols. $W_O = 1$ (circles), $W_O = 2.5$ (squares), $W_O = 4$ (triangles).

they could have scored using the MEG solution for the stochastic setting model. The expected efficiencies are high for all observers and stable across all conditions, indicating that observers were able to take the exogenous variability into account in making capture width settings. The mean efficiency (relative to the stochastic setting model) for the average observer across the conditions is in excess of 87 per cent.

In figure 6, the data for the human observers are regressed against the data obtained from the MEG solution for the stochastic setting model. We first fitted the data with a model of the form:

$$\theta_C = \alpha\theta_C^{MEG} + \beta. \tag{3.5}$$

This analysis resulted in the fit ($\alpha = 1.022$, $\beta = -1.719$) with $r^2 = 0.834$. However, the constant term in the fit was not significantly different from 0 ($t = -0.285$, $p = 0.781$). The data were therefore refitted with a model with no constant term:

$$\theta_C = \alpha\theta_C^{MEG}. \tag{3.6}$$

This analysis resulted in the fit[2] ($\alpha = 0.982$) with α not significantly different from 1 and the 95% CI for α was (0.934, 1.029).

4. DISCUSSION

In this study, we investigated the ability of human observers to (i) recover variability information from an exogenous source and (ii) use this information to choose between possible courses of action. The data from this experiment suggest that humans can indeed estimate and compensate for the uncertainty of an external moving source whose movement is only partially predictable. This finding complements the results of several studies (e.g. [8]) that have inferred that observers must have access to an appropriate estimate of internal motor uncertainty in perceptuo-motor decision-making and can use this to make appropriate rapid pointing movements.

The results regarding recovery of uncertainty information replicate and extend findings from Graf *et al.* [18], in which explicit estimation of visual motion variability was also addressed. The task given to observers in [18] was less well defined than the task used in the current study. In [18], observers were instructed to adjust the length of the (linear) catcher until it was at the smallest size for which they were 'confident' it would catch the dot. Clearly, this instruction is open to interpretation regarding what is meant by 'confident'. Here, we avoid this problem by assigning a points reward for each catcher size and asking the observer to score as many points as possible. The observer's winnings are an objective measure of how well they carried out the task. The points manipulation (together with the bonus prize given for scoring most points) had another benefit in that it is also likely to have increased motivation in the experiment. This was a further potential problem in the study of Graf *et al.* [18], where no feedback was given (the observer never saw the outcome of the extrapolation judgement).

The fact that we replicate the findings of Graf *et al.* [18] in the present experiment (in spite of these changes in methodology) provides compelling evidence that observers can recover an estimate of external motion variability that is tightly coupled to the actual variability in the exogenous source. This can be summarized in stating that human observers appear to know precisely how much more variable one path is than another.

The decision-making analysis undertaken indicated that observers are able to use the variability information recovered from the motion trajectory appropriately to inform decision-making about the size of the catcher. This is particularly evident when we take into account the noise in observer estimates of where the dot will emerge relative to the point at which it hit the inner edge of the occluder. In fact we found that, in this case, observer performance was very close to the MEG solution under the assumptions of a bounded model. Our work leaves open the question as to how observers carry out the task. How do they combine fallible visual estimates across the visible part of the object trajectory and use them to select a capture region? A full understanding of human visual and cognitive capabilities in such tasks requires that we go beyond measures of performance and develop plausible process models as well [22].

One possible outcome in any decision task is that changes in EG associated with even large changes in decision strategy may have negligible effect on the decision-maker's winnings. If the EG function has a 'flat maximum' [23], then observers may exhibit biases in their settings that have little or no effect on their expected winnings. However, the observers' settings in figure 5*a* are evenly distributed around the corresponding maxima, suggesting that observers were sensitive to the gradient of reward present. It is still possible that if we increased the reward values then their performance would improve even further, and consequently we regard our estimates of human ability to be conservative.

It is common in economic decision-making tasks that individual performance is best described using a model that incorporates biased representations of both value and probability [24]. Conversely, the fact that our observers' performance was close to the (bounded) MEG solution suggests that they were able to use unbiased

representations of probability and value. How do we reconcile these results?

The first issue to consider here is that in the present experiment the probabilities are not provided explicitly in numerical forms. It may well be the case that decision-makers are biased in the representation of explicitly presented probabilities, but they are able to encode and use probability information appropriately when it is obtained more naturally via experience [25]. Second, in economic decision-making experiments, participants commonly make small numbers of 'single shot' decisions about large values. In contrast, in the present study, observers make many choices between small values. The representation of small values will naturally tend to be less biased, but also when making many choices economic decision makers tend to become less biased (closer to MEG) [26].

To conclude, we suggest that it is important for the visual system to be able to estimate the external variability in the movement of objects in the environment and use this information to aid in the choice between actions, which involve interaction with or avoidance of that object. When taken together with the results of studies that have examined ability to account for endogenous variability, this study suggests that human observers are finely tuned to uncertainty in general and can exploit this information to guide action.

The study was approved by the local ethics committee at Cardiff University.

This study was partially supported by grants from NIH/NEI (EY019889) and the Humboldt Foundation.

ENDNOTES

[1]We use a polar coordinate system (r, θ) centred on the starting point.

[2]The goodness-of-fit measure (r^2) is a comparison between a fit with only a constant term and a fit with additional terms. Consequently, it is not defined for a regression without intercept.

REFERENCES

1 Verghese, P. & McKee, S. P. 2002 Predicting future motion. *J. Vis.* **2**, 413–423. (doi:10.1167/2.5.5)

2 Watamaniuk, S. N. J. & McKee, S. P. 1995 Seeing motion behind occluders. *Nature* **377**, 729–730. (doi:10.1038/377729a0)

3 Scholl, B. J. & Pylyshyn, Z. W. 1999 Tracking multiple items through occlusion: clues to visual objecthood. *Cogn. Psychol.* **38**, 259–290. (doi:10.1006/cogp.1998.0698)

4 Makin, A., Poliakoff, E. & El-Deredy, W. 2009 Tracking visible and occluded targets: changes in event related potentials during motion extrapolation. *Neuropsychologia* **47**, 1128–1137. (doi:10.1016/j.neuropsychologia.2009.01.010)

5 Pola, J. & Wyatt, H. 1997 Offset dynamics of human smooth pursuit eye movements: effects of target presence and subject attention. *Vision Res.* **37**, 2579–2595. (doi:10.1016/S0042-6989(97)00058-8)

6 Becker, W. & Fuchs, A. F. 1985 Prediction in the oculomotor system: smooth pursuit during transient disappearance of a visual target. *Exp. Brain Res.* **57**, 562–575.

7 Bennett, S. J. & Barnes, G. R. 2003 Human ocular pursuit during the transient disappearance of a visual target. *J. Neurophysiol.* **90**, 2504–2520. (doi:10.1152/jn.01145.2002)

8 Trommershäuser, J., Maloney, L. T. & Landy, M. S. 2008 Decision making, movement planning and statistical decision theory. *Trends Cogn. Sci.* **12**, 291–297. (doi:10.1016/j.tics.2008.04.010)

9 Maloney, L. T. & Zhang, H. 2010 Decision-theoretic models of visual perception and action. *Vision Res.* **50**, 2362–2374. (doi:10.1016/j.visres.2010.09.031)

10 Trommershäuser, J., Maloney, L. T. & Landy, M. S. 2003 Statistical decision theory and the selection of rapid, goal-directed movements. *J. Opt. Soc. Am. A* **20**, 1419–1433. (doi:10.1364/JOSAA.20.001419)

11 Trommershäuser, J., Maloney, L. T. & Landy, M. S. 2003 Statistical decision theory and trade-offs in the control of motor response. *Spat. Vis.* **16**, 255–275. (doi:10.1163/156856803322467527)

12 Wu, S.-W., Delgado, M. R. & Maloney, L. T. 2009 Economic decision-making under risk compared with an equivalent motor task. *Proc. Natl Acad. Sci. USA* **106**, 6088–6093. (doi:10.1073/pnas.0900102106)

13 Hudson, T. E., Maloney, L. T. & Landy, M. S. 2008 Optimal compensation for temporal uncertainty in movement planning. *PLoS Comput. Biol.* **4**, e10000130. (doi:10.1371/journal.pcbi.1000130)

14 Dean, M., Wu, S. & Maloney, L. 2007 Trading off speed and accuracy in rapid, goal-directed movements. *J. Vis.* **7**, 1–12. (doi:10.1167/7.5.10)

15 Battaglia, P. W. & Schrater, P. R. 2007 Humans trade off viewing time and movement duration to improve visuomotor accuracy in a fast reaching task. *J. Neurosci.* **27**, 6984–6994. (doi:10.1523/jneurosci.1309-07.2007)

16 Wu, S.-W., Dal Martello, M. F. & Maloney, L. T. 2009 Sub-optimal allocation of time in sequential movements. *PLoS ONE* **4**, e8228. (doi:10.1371/journal.pone.0008228)

17 Zhang, H., Wu, S. & Maloney, L. 2010 Planning multiple movements within a fixed time limit: the cost of constrained time allocation in a visuo-motor task. *J. Vis.* **10**, 1–17. (doi:10.1167/10.6.1)

18 Graf, E. W., Warren, P. A. & Maloney, L. T. 2005 Explicit estimation of visual uncertainty in human motion processing. *Vision Res.* **45**, 3050–3059. (doi:10.1016/j.visres.2005.08.007)

19 Evans, M., Hastings, N. & Peacock, B. 2000 von Mises distribution. In *Statistical distributions,* 3rd edn, ch. 41. pp. 189–191. New York, NY: Wiley.

20 Fisher, N. I. 1993 *Statistical analysis of circular data*. Cambridge, UK: Cambridge University Press.

21 Howes, A., Lewis, R. L. & Vera, A. 2009 Rational adaptation under task and processing constraints: implications for testing theories of cognition and action. *Psychol. Rev.* **116**, 717–751. (doi:10.1037/a0017187)

22 Bogacz, R., Brown, E., Moehlis, J., Holmes, P. & Cohen, J. D. 2006 The physics of optimal decision making: a formal analysis of models of performance in two-alternative forced choice tasks. *Psychol. Rev.* **113**, 700–765. (doi:10.1037/0033-295X.113.4.700)

23 von Winterfeldt, D. & Edwards, W. 1982 Costs and payoffs in perceptual research. *Psychol. Bull.* **91**, 609–622. (doi:10.1037/0033-2909.91.3.609)

24 Kahneman, D. & Tversky, A. 1979 Prospect theory: an analysis of decisions under risk. *Econometrica* **47**, 263–291. (doi:10.2307/1914185)

25 Hertwig, R., Barron, G., Weber, E. U. & Erev, I. 2004 Decisions from experience and the effect of rare events in risky choice. *Psychol. Sci.* **15**, 534–539. (doi:10.1111/j.0956-7976.2004.00715.x)

26 Redelmeier, D. A. & Tversky, A. 1992 On the framing of multiple prospects. *Psychol. Sci.* **3**, 191–193. (doi:10.1111/j.1467-9280.1992.tb00025.x)